15/02/2020

The rotationally resolved symmetric 2OH excitation in H_2O-CO_2 observed using pulsed supersonic expansion and CW-CRDS

To be submitted to Chemical physics letters

A. S. Bogomolov[1,2], A. Roucou[3], R. Bejjani[3], M. Herman[4],

N. Moazzen-Ahmadi[5], C. Lauzin[3]

[1] Institute of Chemical Kinetics and Combustion, Institutskaya Str. 3,
Novosibirsk, Russia

[2] Novosibirsk State University, Pirogova Str. 2, Novosibirsk, Russia

[3] Institute of Condensed Matter and Nanosciences, Université catholique
de Louvain, B-1348, Louvain-la-Neuve, Belgium.

[4] Spectroscopy, Quantum Chemistry and Atmospheric Remote Sensing
(SQUARES), Faculté des Sciences, Université libre de Bruxelles (ULB), 50 ave.
F-D Roosevelt, B-1050, Brussels, Belgium

[5] Department of Physics and Astronomy, University of Calgary, 2500
University Drive North West, Calgary, Alberta T2N 1N4, Canada

Pages: 15

Tables: 2

Figures: 4

Send mail to Prof. C. Lauzin

Email: clement.lauzin@uclouvain.be

Abstract

The rovibrational band corresponding to a double excitation of the OH symmetric stretch of the H_2O unit in the H_2O-CO_2 van der Waals complex has been recorded using CW-CRDS and a pulsed slit expansion seeded with He. The set-up is presented. The rotational analysis of this band is detailed and the results of the global fit of these data with those of the other 2OH excitation band and of the ground vibrational states are reported including data from the literature. The tunneling frequency and the vibrational predissociation lifetime are shown to decrease with vibrational excitation.

1. **Introduction**

H-bonded and van der Waals molecular complexes have been the subject of constant interest in the literature to fill the gap between gas and condensed phases [1-3], to study intramolecular chemistry [4-6] and to investigate anomalous energy level structures [7]. Today, this interest is further supported by atmospheric and planetary motivations [8-12].

The H_2O-CO_2 van der Waals complex which we investigate in the present work is the first step in the solvation process of carbon dioxide and is an intermediate species on the reaction coordinate leading to the formation of carbonic acid (H_2CO_3) [13,14]. It demonstrates interesting intermolecular dynamics. It is also predicted to be one of the most abundant neutral hydrated complexes in our atmosphere [15].

H_2O-CO_2 has been studied in the microwave range [16,17] and the (001) ← (000) [18] and (010) ← (000) [19] transitions were investigated in the mid-infrared range, with transitions labeled in terms of the (v_1,v_2,v_3) vibrational quantum numbers of the isolated water molecule. This complex was also studied in Ne matrices in the far-infrared [20] and mid-infrared [21] ranges and in N_2 matrices in the far-infrared region [22]. The intermolecular interaction between water and carbon dioxide was studied theoretically using *ab initio* methods by various authors (*e.g.* [23,24]).

H_2O-CO_2 presents a C_{2V} symmetry in which the two molecules are linked through an intermolecular bond between the O of H_2O and the C of CO_2, defining the *a* principal axis of inertia, with calculated interaction/dissociation energies of De/D_0 = 1053/787 cm^{-1} [24]. A more complete symmetry analysis requires considering the G_8 symmetry group, thus including internal rotation resulting from the permutation of the two hydrogens (or equivalently the two oxygens). This movement is indeed considered as *feasible* with a barrier predicted to be around 287 cm^{-1} [17] . This internal rotation gives rise to a tunneling splitting of each ro-vibrational energy level into two components, with only one of them populated for each K_a parity, where K_a is the projection of the total angular momentum on the *a* principal inertial axis. Each tunneling component is associated to one nuclear spin isomer with statistical weights 1 and 3 for K_a even and odd, respectively as detailed in ([17,25]).

We already, recently reported on the high-resolution absorption spectrum of the H_2O-CO_2 van der Waals complex in the doubly excited OH stretch region (7240 cm^{-1}) [25]. The observation of two bands can be expected in this range, leading to transitions from the ground state to (200) (of *a*-type *i.e.* with ΔK_a even and ΔK_c odd) and to (101) (of *b*-type *i.e.* with ΔK_a and ΔK_c odd), with origins close to those in the water monomer, *i.e.* 7201.5 and 7249.8 cm^{-1}, respectively. The region instrumentally accessible at the time of these previous experiments was, however, limited to 7230 – 7260 cm^{-1} due to restricted available laser coverage, thus forbidding the observation of the lower energy band. Nevertheless, this previous investigation unexpectedly demonstrated the presence of two vibrational bands. As discussed in [25], both bands involve H_2O rather than CO_2 excitation. One of them was assigned to the (101) ← (000) vibrational excitation. This assignment was based on the proximity in energy with the monomer band origin (red shift of 3 cm^{-1}) and on the observation of the expected *b*–type rotational structure. The second band, with origin at 7237.6 cm^{-1} could not be assigned to (200). It is indeed 36 cm^{-1} blue shifted from the expected (200) value and shows *b*-type rather than the expected *a*-type structure. It was assigned as a combination band involving (200) and the lowest frequency intermolecular CO_2 libration, ν_{12} as calculated *ab initio* by Wang and Bowman [24] and Andersen *et al.* [20]. Transition to (200)+ ν_{12} is expected to lead to a *b*-type band, as observed. The similar intensity observed for the two bands on the spectrum was explained through a Fermi-type resonance mixing the (200)+ ν_{12} and (101) upper states. This assignment was presented as tentative until an *a*-type band could be reported, with intensity similar to that to (101) and with origin close to 7201.5 cm^{-1}, to be assigned to (200). The aim of this work is to report on this observation.

The previous spectrum was recorded using the FANTASIO+, CW-cavity ring-down (CW-CRDS) spectrometer built and located at the Université libre de Bruxelles (ULB) [26]. We have again used this set-up, now moved to the Université catholique de Louvain (UCLouvain), using another DFB laser source to extend the wavelength range available and search for the expected (200)←(000) band. We also improved the set-up, resulting in a factor 2 increase of the signal-to-noise ratio (S/N), using a pulsed, rather than a continuous slit nozzle and a dedicated sampling procedure. It is described in the next section. The spectral analysis is detailed and discussed in section 3. It includes a global fit of the data on the (200) state from the present work, on (101) from our previous study [25], and data on the ground vibrational state from the microwave literature [17].

2. Experimental procedure

The high-resolution spectrum of H_2O-CO_2 was recorded using (CW-CRDS) spectroscopy and the FANTASIO+ set-up [26]. The cavity mirrors are mounted on a vacuum chamber pumped by two turbomolecular pumps with total pumping speed of 6400 l/s. The relative wavenumber scale is obtained by linearization of the frequency scale of spectra using the maxima of interference fringes from an evacuated Fabry-Pérot etalon fixed on an invar rod. The wavenumber scale is then absolutely calibrated using water monomer lines positions from the HITRAN database [27]. The measurement precision and accuracy are both estimated to 10^{-3} cm^{-1}. Further information on FANTASIO+ is available in the literature [26]. This set-up has been moved from ULB to UClouvain and a previously missing DFB laser source was used to record the (200)←(000) vibrational transition of the water monomer in the H_2O-CO_2 complex.

We took this opportunity to implement a pulsed slit supersonic expansion, allowing the use of He as seeding gas. The gas mixture was composed of CO_2 0.86% and He as carrier gas and was bubbled through H_2O. The slit was assembled from pulsed Parker series 9 valve driven by IOTA ONE power supply, and a home-made multichannel block with 30 mm long and 50 µm spaced jaws similar to those developed in Calgary [28]. The valve operates typically at 5 Hz with 30 ms pulse duration that allowed us increasing backing pressure up to 3 bar and using He as seeding gas, instead of, previously [25], less than 1 bar and Ar, respectively.

Unexpectedly, the temperature estimated to be 15 K from the rotational structure of the recorded band, was not significantly decreased using this new pulsed He rather than the CW Ar seeded expansion [25].

Ringdowns are sorted following that the molecular beam is ON or OFF using TTL signal from the valve driver as illustrated in Figure 1.

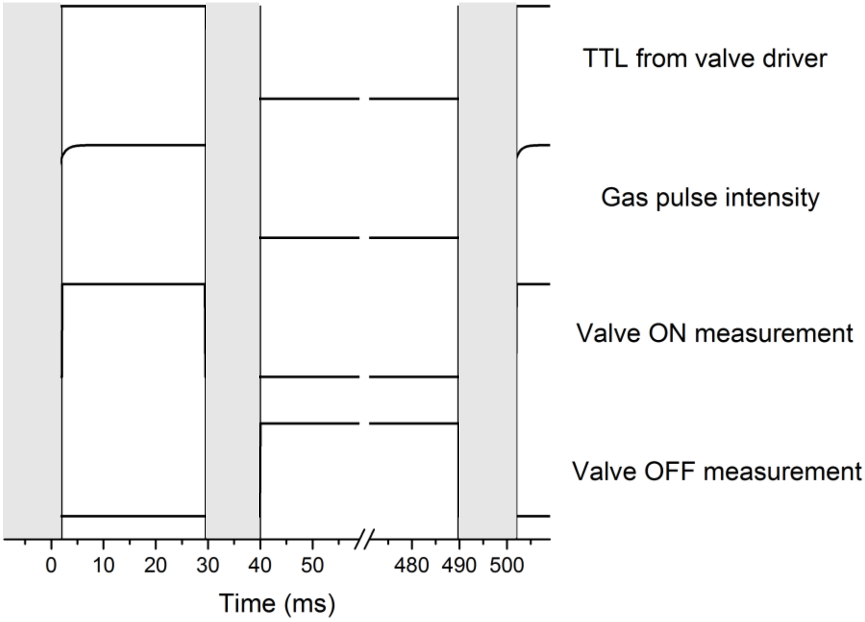

Figure 1: Illustration of the data recording sequence in the pulsed jet used to investigate H_2O-CO_2, the grey areas are measurement dead periods which allow to discriminate between gas pulse ON and OFF.

The ringdowns ON/OFF were measured in between 2/40 and 29.5/190 ms after the TTL rise. These tunable time windows were implemented using an Arduino Uno and programmed digital logic gates. All other ring-down events were rejected due to unstable molecular beam conditions leading to the appearance of excessive noise on the baseline when one is making the difference between the inverse of ringdowns times for beam ON and OFF. The resulting improvement in S/N is estimated to be a factor 2 for the same measurement time. As with previous experiments reported using FANTASIO+, the rotational analysis demonstrated no sign of nuclear spin relaxation in the expansion [29].

3. Results

The newly observed band with origin at 7195.4 cm^{-1} is presented in Figures 2 and 3. It is thus close to the (200)←(000) vibrational excitation in the monomer (6.1 cm^{-1} red-shift), with the required *a*-type structure and has similar intensity as that of (101). It can thus be reliably assigned to the symmetric 2OH excitation in H_2O-CO_2, i.e. (200)←(000).

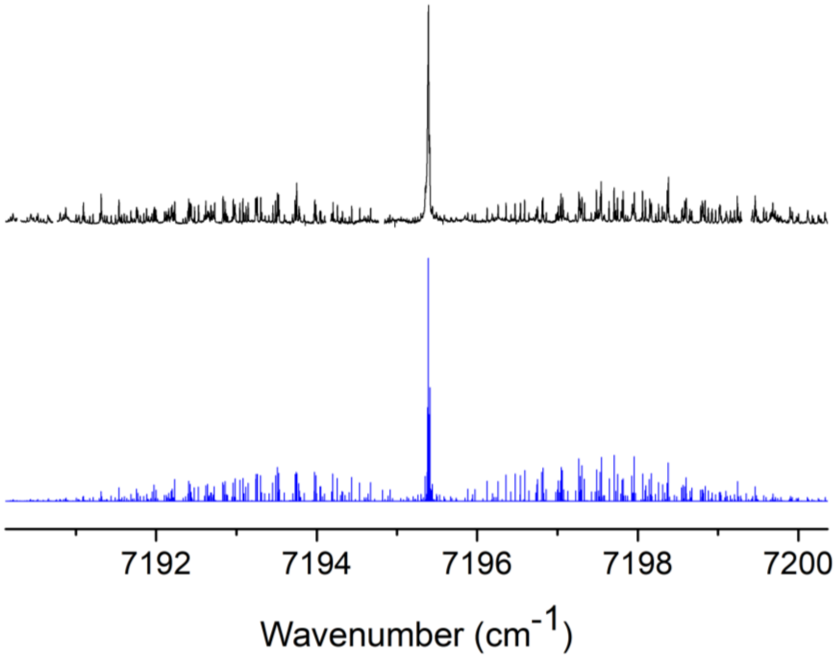

Figure 2: Experimental spectrum (top) and simulation (bottom) of (200)←(000) in H_2O-CO_2. The simulation used the spectroscopic parameters from Table 1 and a rotational temperature of 15 K.

As pointed out in the introduction, a single nuclear spin isomer needs to be considered for each K_a parity. The rotational analysis was thus performed separately for each isomer, using an asymmetric-top Watsonian [30] in the A reduction as implemented in the PGOPHER software [31]. The resulting assignments are listed in the supplementary materials.

The list of assigned lines shows that the present analysis involves values of the rotational quantum numbers with $J''\leq19$ and $K_a''\leq6$. This is significantly higher than the microwave data in the ground state [17], in which $J''\leq6$ and $K_a''\leq4$. A global least-squares fit procedure combining the assignments was performed for (200), (101) and the ground state, using data from the present work, refs [25] and [17]. A weight proportional to the precision of the line measurement was given to each set of data. The 455 transition frequencies were used to fit 58 parameters, with a root mean square (RMS) value of 7.10^{-4} cm^{-1} (210 MHz) and 2 kHz for the overtone and microwave data, respectively. The resulting rotational constants for the ground, (200) and (101) states are listed in Table 1, together with their estimated uncertainty. Thanks to the global fit, those for (101) state are slightly modified compared to Table 2 in [25]. The excellent agreement between observed and simulated spectra for the (200)←(000) band is illustrated in Figure 3.

Concerning the microwave data, Columberg *et al.* [17] considered each K_a parity separately and developed a specific Hamiltonian taking into account the relaxation of the intermolecular distance during the internal rotation process. This Hamiltonian provided physical insights on the tunnelling process but was not mandatory to reproduce the measured line positions within experimental accuracy. The present, near infrared, data include significantly higher J, K_a values in the ground state and we found it adequate to use the same Watsonian to fit the rotational constants for all three states involved to improve the determination of the spectroscopic parameters. The band assigned to $(200)+\nu_{12} \leftarrow (000)$ in [25] was not included in this global fit because of the presence of various unraveled perturbations in this combination band.

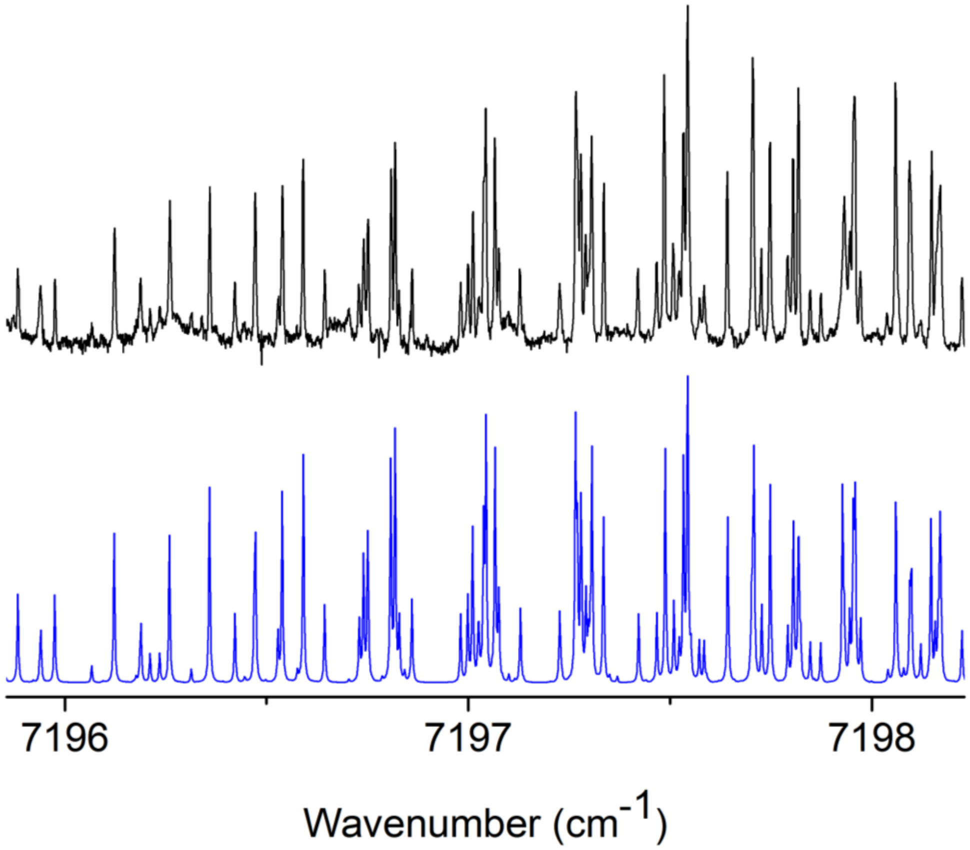

Figure 3: Zoom in the (200)←(000) band of H_2O-CO_2 illustrating the agreement between experimental (top) and simulated (bottom) spectra using the constants in Table 1 and a rotational temperature of 15 K.

	Ground state		**(200)**		**(101)**	
	K_a even	***K_a odd***	**K_a even**	***K_a odd***	***K_a even***	***K_a odd***
ν_0/cm^{-1}			**7195.41414(20)**	**7195.39732(14)**	**7246.89497(19)**	**7247.08961(15)**
A/cm^{-1}	**0.3840905(12)**	**0.383647(12)**	**0.383769(48)**	**0.383390(18)**	**0.385458(19)**	**0.385513(13)**
B/cm^{-1}	**0.155921933(44)**	**0.15594370(22)**	**0.1559404(98)**	**0.1559425(40)**	**0.155130(12)**	**0.155134(13)**
C/cm^{-1}	**0.110220986(46)**	**0.11023029(21)**	**0.1101880(88)**	**0.1101971(45)**	**0.109583(13)**	**0.1097569(92)**
$\Delta_K/10^{-5}$cm^{-1}	**-1.054(31)**	**-1.046(37)**	**-1.63(39)**	**-1.191(44)**	**-0.626(73)**	**-0.82(10)**
$\Delta_{JK}/10^{-5}$cm^{-1}	**1.11650(14)**	**1.1154(14)**	**1.169(59)**	**1.1965(86)**	**0.683(49)**	**0.961(84)**
$\Delta_J/10^{-7}$cm^{-1}	**9.4785(21)**	**9.454(23)**	**10.04(42)**	**9.42(13)**	**9.26(83)**	**11.2(13)**
$\delta_K/10^{-6}$cm^{-1}	**7.833(13)**	**7.72(11)**	**6.29(62)**	**8.07(20)**	**13.6(14)**	**13.1(21)**
$\delta_J/10^{-7}$cm^{-1}	**2.8232(16)**	**2.81894(82)**	**3.51(26)**	**2.902(86)**	**3.35(61)**	**2.12(55)**

Table 1: Spectroscopic parameters for the ground, (200) and (101) states of H_2O-CO_2 resulting from a global fit procedure (cm^{-1}). Uncertainties in parentheses are 1σ from the least-squares fit. This fit reproduces the observed line positions with a root mean square (RMS) value of 7.10^{-4} cm^{-1} (210 MHz) and 2 kHz for the overtone and microwave data, respectively.

The results do not show any evidence for local perturbations. The procedure to estimate the upper state vibrational predissociation lifetime from the experimental linewidths, as described in [32], was applied to the present data. It led to values of the order of 1.0 ns from all lines in (200). This value does not differ to that in (101) nor in (200)+ν_{12} [25]. The predissociation lifetime is thus, as expected, shorter than that for (001), estimated by Block *et al.*[18] to lie between 100 ns and 200 μs.

The difference between the (200) and (200)+ ν_{12} band origins in H_2O-CO_2 allows refining the value of ν_{12} to 42.2 cm^{-1}, neglecting the contribution of anharmonicity ($x_{i,j}$). $x_{1,12}$ can actually be expected to be very small, typically 1% of the lowest frequency mode [33], thus less than 1 cm^{-1}.

Trends in the evolution of the tunneling dynamics with vibrational excitation in H_2O-CO_2 can be obtained by subtracting band origins ($J''=J'=0$) for *Ka"* even and *Ka"* odd, $\Delta\nu_0 = \nu_0(K_a \text{ even}) - \nu_0(K_a \text{ odd})$. *Ka"* even and *Ka"* odd values are associated to two different nuclear spin isomers, i.e. to two different molecules in a one to three proportion. It can be shown, see Fig. 4, that $\Delta\nu_0$ corresponds to the sum (for *b*-type) or difference (for *a*-type) of the energy splittings due to tunneling in the ground (S") and excited (S') states. The splittings for all studied vibrational states are reported in Table 2. The value of S' can be calculated assuming S"= 0.1356 cm^{-1} [17,18]. This value was derived from microwave [17] and infrared [18] studies and found to be in good agreement with the *ab initio* prediction [24] of the height of the potential barrier for internal rotation.

Figure 4: Procedure for retrieval of tunneling splittings in excited (S') vibrational states in H_2O-CO_2. The physical meaning of the band origins, determined from the fit procedure, depicted as dashed arrow in the figure, is presented for *a*-type transitions in panel a) and for *b*-type in panel b). In both cases non-existing levels are displayed transparently and the statistical weight is given in parenthesis.

Vibrational state	$\Delta\nu_0 = \nu_0(K_a$"even)-$\nu_0(K_a$"odd)	Splitting combinations	S', considering S" = 0.1356(13) cm^{-1} [e]
(010)[a]	0.0070(2)	S"-S'	0.129(2)
(001)[b]	0.268(1)	S"+S'	0.133(2)
(200)[c]	0.0168(3)	S"-S'	0.119(2)
(101)[d]	0.1948(3)	S"+S'	0.059(2)
(200)+ν_{12}[d]	0.1246(5)	S"+S'	-0.011(2)

[a] from [19], [b] from [18], [c] This work, [d] from [25], [e] from [17,18].

Table 2: Tunneling splittings in excited vibrational states (S') in H_2O-CO_2, as calculated from $\Delta\nu_0 = \nu_0(K_a$ even) - $\nu_0(K_a$ odd) values reported in the literature.

The S' values of (001) and (010) are equivalent within error bars and are lower than the value for the ground state. S' further decreases for (200) and even more dramatically for (101) and (200)+ν_{12}. The value of S' associated with this combination state should, however, be taken cautiously since the presence of severe perturbations in the band makes the related rotational parameters less reliable [25]. In any case, S' shows a decrease with vibrational excitation. Intramolecular excitation seems thus to hinder the tunneling dynamics, as observed for other dimers (i.e. $(C_2D_2)_2$ [34] and $(HF)_2$ [35]).

In conclusion, the (200)←(000) vibrational band in H_2O-CO_2 has been observed around the related excitation in the H_2O monomer, thus supporting the vibrational assignment of two additional bands previously reported in the same excitation range, (101)←(000) and (200)+ ν_{12}←(000). The frequency of the ν_{12} mode has been refined to 42.2 cm^{-1}. A set of rotational constants has been fitted simultaneously for (101), (200) and the ground vibrational states, providing RMS values of 7.10^{-4} cm^{-1} (210 MHz) and 2 kHz for the overtone and microwave data, respectively. The hindering of the tunnelling dynamics with the vibrational excitation has been highlighted. A shortening of the vibrational predissociation lifetime with the number of quanta of vibrational excitation has been confirmed, with no dependence on the nature of the OH stretch involved. Finally, we highlighted the changes in the FANTASIO+ set-up, now using a pulsed slit and He gas in the expansion. These changes with further modifications will hopefully allow to observe larger clusters and more fragile complexes.

Acknowledgments

A.B. thanks the financial support of Wallonie-Bruxelles international (WBI) and Uclouvain. A.R thanks the support of WBI (session 2019). C.L. thanks the FNRS (under Grants n: J.0179.18, J.0129.20 and IISN convention n°4.4504.10) and the Communauté Française de Belgique (ARC IBEAM 18/23-090) for financial support. R.B. thanks UcLouvain for FSR PhD fundings. C.L. warmly thanks the Service SQUARES of ULB for the loan of the FANTASIO+ set-up. N.M. thanks the financial support of the Natural Sciences and Engineering Research Council of Canada.

References

[1] F.N. Keutsch, R.J. Saykally, Proceedings of the National Academy of Sciences of the United States of America 98 (2001) 10533.

[2] J.N. Oliaee, M. Dehghany, N. Moazzen-Ahmadi, A.R.W. McKellar, Physical Chemistry Chemical Physics 13 (2011) 1297.

[3] A.R.W. McKellar, Y. Xu, W. Jager, Physical Review Letters 97 (2006) 183401/1.

[4] F. Madeja, M. Havenith, Journal of Chemical Physics 117 (2002) 7162.

[5] D.J. Nesbitt, Chemical Reviews 112 (2012) 5062.

[6] C.T. Wolke, J.A. Fournier, L.C. Dzugan, M.R. Fagiani, T.T. Odbadrakh, H. Knorke, K.D. Jordan, A.B. McCoy, K.R. Asmis, M.A. Johnson, Science 354 (2016) 1131.

[7] A. Barclay, A. van der Avoird, A. McKellar, N. Moazzen-Ahmadi, Physical Chemistry Chemical Physics 21 (2019) 14911.

[8] M.Y. Tretyakov, E. Serov, M. Koshelev, V. Parshin, A. Krupnov, Physical Review Letters 110 (2013) 093001.

[9] T. Odintsova, M.Y. Tretyakov, A. Zibarova, O. Pirali, P. Roy, A. Campargue, Journal of Quantitative Spectroscopy and Radiative Transfer 227 (2019) 190.

[10] K. Pfeilsticker, H. Bösch, C. Camy-Peyret, R. Fitzenberger, H. Harder, H. Osterkamp, Geophysical Research Letters 28 (2001) 4595.

[11] N.S. Shuman, D.E. Hunton, A.A. Viggiano, Chemical reviews 115 (2015) 4542.

[12] R. Wordsworth, Y. Kalugina, S. Lokshtanov, A. Vigasin, B. Ehlmann, J. Head, C. Sanders, H. Wang, Geophysical Research Letters 44 (2017) 665.

[13] T. Mori, K. Suma, Y. Sumiyoshi, Y. Endo, The Journal of Chemical Physics 130 (2009) 204308.

[14] T. Mori, K. Suma, Y. Sumiyoshi, Y. Endo, The Journal of Chemical Physics 134 (2011) 044319.

[15] H.G. Kjaergaard, T.W. Robinson, D.L. Howard, J.S. Daniel, J.E. Headrick, V. Vaida, The Journal of Physical Chemistry A 107 (2003) 10680.

[16] K. Peterson, W. Klemperer, The Journal of Chemical Physics 80 (1984) 2439.

[17] G. Columberg, A. Bauder, N. Heineking, W. Stahl, J. Makarewicz, Molecular Physics 93 (1998) 215.

[18] P.A. Block, M.D. Marshall, L.G. Pedersen, R.E. Miller, Journal of Chemical Physics 96 (1992) 7321.

[19] Y. Zhu, S. Li, P. Sun, C. Duan, Journal of Molecular Spectroscopy 283 (2013) 7.

[20] J. Andersen, J. Heimdal, D. Mahler, B. Nelander, R.W. Larsen, The Journal of Chemical Physics 140 (2014) 091103

[21] P. Soulard, B. Tremblay, The Journal of Chemical Physics 143 (2015) 224311.

[22] X. Zhang, S.P. Sander, The Journal of Physical Chemistry A 115 (2011) 9854.

[23] J. Makarewicz, The Journal of Chemical Physics 132 (2010) 234305.

[24] Q. Wang, J.M. Bowman, The Journal of Chemical Physics 147 (2017) 161714.

[25] C. Lauzin, A. Imbreckx, T. Foldes, T. Vanfleteren, N. Moazzen-Ahmadi, M. Herman, Molecular Physics 118 (2019) 1.

[26] K. Didriche, C. Lauzin, T. Földes, X. de Ghellinck D'Elseghem Vaernewijck, M. Herman, Molecular Physics 108 (2010) 2155.
[27] Q. Kou, G. Guelachvili, M. Abbouti Temsamani, M. Herman, Canadian Journal of Physics 72 (1994) 1241.
[28] J. Norooz Oliaee, PhD, University of Calgary, 2013.
[29] M. Herman, T. Földes, K. Didriche, C. Lauzin, T. Vanfleteren, International Reviews in Physical Chemistry 35 (2016) 243.
[30] J.K.G. Watson, Vibrational Spectra and Structure. A Series of Advances, Elsevier, Amsterdam, 1977.
[31] C.M. Western, B.E. Billinghurst, Physical Chemistry Chemical Physics 19 (2017) 10222.
[32] C. Lauzin, K. Didriche, P. Macko, J. Demaison, J. Liévin, M. Herman, Journal of Physical Chemistry A 113 (2009) 2359.
[33] N. Moazzen-Ahmadi, A. McKellar, International Reviews in Physical Chemistry 32 (2013) 611.
[34] J.N. Oliaee, N. Moazzen-Ahmadi, A. McKellar, Molecular Physics 110 (2012) 2797.
[35] Z. Yu, E. Hammam, W. Klemperer, The Journal of Chemical Physics 122 (2005) 194318.